

# **INTERNATIONAL JOURNAL OF INSTITUTIONAL PHARMACY AND LIFE SCIENCES**

**Life Sciences**

**Research Article.....!!!**

Received; accepted

## **3-D QSAR COMFA, COMSIA AND DOCKING STUDIES ON NOVEL TARTARATE-BASED TNF-ALPHA CONVERTING ENZYME (TACE) INHIBITORS**

Uday Chandra Kumar\* and Mahmood Shaik

Bioinformatics Division, Environmental Microbiology Lab, Department of Botany, Osmania University, Hyderabad 500 007, A.P., India

### **Keywords:**

Comparative Molecular Field Analysis; Comparative Molecular Similarity Indices Analysis; 3D-QSAR; Non-hydroxamate tryptophan sulfonamide; TNF-alpha converting enzyme

### **For Correspondence:**

**Uday Chandra Kumar**

Bioinformatics Division,  
Environmental Microbiology  
Lab, Department of Botany,  
Osmania University,  
Hyderabad 500 007, A.P.,  
India

E-mail:

[dr.udaynair16@gmail.com](mailto:dr.udaynair16@gmail.com)

### **ABSTRACT**

Comparative Molecular Field Analysis (COMFA) and Comparative Molecular Similarity Indices Analysis (CoMSIA) was performed on a series of non-hydroxamate tryptophan sulfonamide derivatives as inhibitors of TNF-alpha converting enzyme. Ligand molecular superimposition on the template structure was performed by the atom/ shape based root mean square fit and database alignment methods. There are no outliers in the training set of 61 molecules which improved the predictivity of the model. The statistically significant model was established of 61 molecules, which were validated by a test set of 12 molecules. The atom and shape based root mean square alignment yielded the best predictive COMFA model  $r^2_{cv} = 0.844$ ,  $r^2_{\text{Leave one out}} = 0.861$ ,  $r^2_{nv} = 0.979$ , Boot strap=mean=0.987, std dev=0.004, F value = 482.776, standard error of estimate = 0.181 while the CoMSIA model yielded  $r^2_{cv} = 0.759$ ,  $r^2_{\text{Leave one out}} = 0.776$ ,  $r^2_{nv} = 0.987$ , Boot strap=mean=0.993 std dev=0.003, F value = 628.811 and standard error of estimate = 0.145.

## INTRODUCTION

TNF-alpha converting enzyme (TACE) is the metalloproteinase that processes the 26 kDa membrane bound precursor of TNF-alpha (proTNF-alpha) to the 17 kDa soluble component. Although a number of proteases have been shown to process proTNF-alpha, none do so with the efficiency of TACE. A series of orally bioavailable, selective, and potent TACE inhibitors are currently in clinical development. These inhibitors effectively block TACE mediated processing of proTNF-alpha and can reduce TNF production by lipopolysaccharide stimulated whole blood by >95%. Through a series of studies it is shown here that >80% of the unprocessed pro TNF-alpha is degraded intracellularly. The remainder appears to be transiently expressed on the cell surface. Although, in vitro, TACE inhibition has also been implicated in shedding of p55 and p75 surface TNF-alpha receptors, the in vivo data cast doubt on the consequences of this finding. In a mouse model of collagen induced arthritis, the inhibitors are efficacious both prophylactically and therapeutically. The efficacy seen is equivalent to strategies that neutralize TNF-alpha. In many studies greater efficacy is observed with the TACE inhibitors, presumably owing to greater penetration to the site of TNF-alpha production.

The activity of TACE is regulated at three distinct levels: transcription of the gene, pro-enzyme activation, and through specific interaction with its physiological inhibitor tissue inhibitor of metalloproteinase 3 (TIMP3), a member of a family of endogenous matrix metalloproteinase inhibitors (1-3). TIMP3, a secreted 24-kDa protein which binds to the extracellular matrix, may be a critical regulator of the inflammatory response and a potential therapeutic protein to control inflammation through a reduction in the amount of secreted TNF. Thus, TACE inhibition may represent a novel approach to treat inflammation, and consequently, a large number of synthetic TACE inhibitors have been reported (4-6).

## MATERIALS AND METHODS

All Structures, molecular modeling and 3D-QSAR studies were performed on SYBYL 6.7 with TRIPOS Force Field on a Silicon Graphics O2 workstation with IRIX operating system. Energy minimizations were performed using the Tripos force field and the Gasteiger-Huckel charge

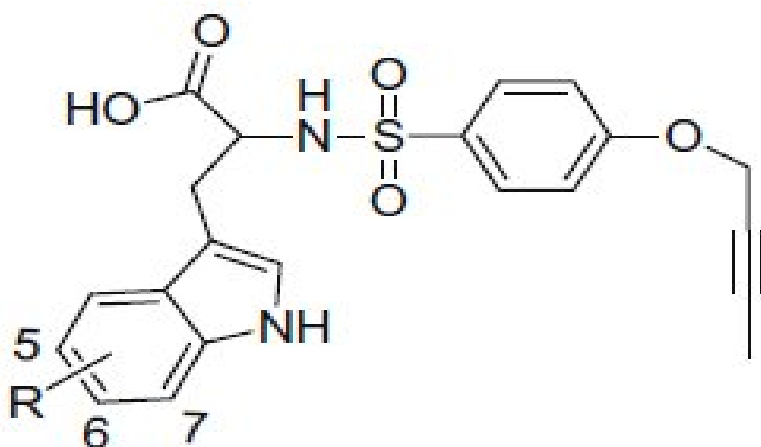
with a distance-dependent dielectric and Powell conjugate gradient algorithm. The criterion of convergence was 0.05 kcal/mol. Subsequently, the lowest-energy conformation found for each structure was submitted to optimization with the semi-empirical program MOPAC 6.0 and applying the AM1 Hamiltonian. All the molecules were constructed using a grid having a spacing of 1.54 Å between grid points. This is the default spacing, which represents sp<sup>3</sup> carbon-carbon bond length. The molecules were cleaned up and quick minimized after sketching. Because no experimental data on the biologically relevant conformations of the selected compounds were available (for example, atomic coordinates derived from X-ray crystallographic studies of their complexes with the putative receptor), we resorted to a general molecular mechanics approach (AM1) to build the conformational models to be used for generation of CoMFA models. A chirality check was performed to identify chiral atoms, after adding hydrogen's, it was important to consider all possible enantiomers as the activity was reported for racemic mixtures. Then the molecules were subjected for energy minimization (geometry optimization) at a gradient of 1.0 kcal/mol with delta energy change of 0.001 kcal/mol with the TRIPOS standard force field.

### **Dataset and molecular modeling**

A series of 76 synthetic non-hydroxamate tryptophan sulfonamide derivatives were considered with their biological activities. The biological activity is given as IC<sub>50</sub> which is converted to pIC<sub>50</sub> using the following formula  $pIC_{50} = \log (1/IC_{50})$ , where IC<sub>50</sub> is the molar concentration of TACE necessary to give half-maximum inhibition.

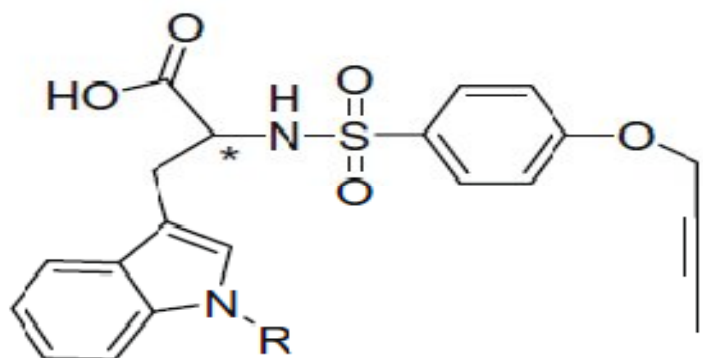
All the calculations were performed on a Silicon Graphics workstation, using Sybyl 6.7.

Table 1. The 76 compounds are shown in the table which is based on this core scaffold



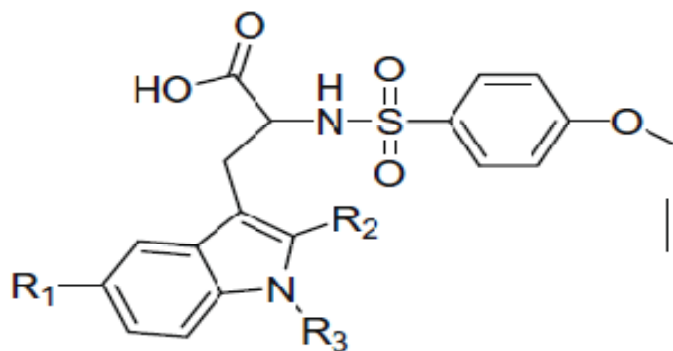
S.NO	COMPOUND	R	IC50
1	8	H,(L)	8.2
2	9	H,(D)	2.53
3	11a	5-Me (racemic)	0.28
4	11b	5-Me (enantiomer-1)	27
5	11c	5-Me (enantiomer-2)b	0.14
6	11d	5-MeO (racemic)	0.36
7	11e	5-MeO (enantiomer-1)	10.1
8	11f	5-MeO (enantiomer-2)b	0.14
9	11g	5-BnO (racemic)	0.75
10	11h	5-BnO (enantiomer-1)	6.98
11	11i	5-BnO (enantiomer-2)b	0.37

12	11j	5-F (racemic)	1.56
13	11k	5-OH (racemic)	1.61
14	11l	5-Br (racemic)	0.63
15	11m	6-F (racemic)	2.96
16	11n	6-Me (racemic)	1.57



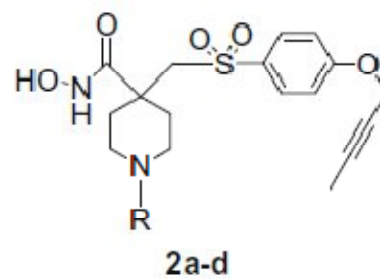
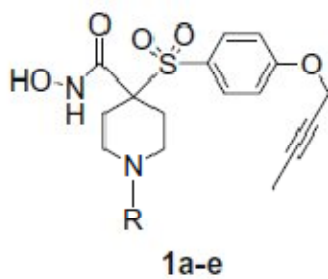
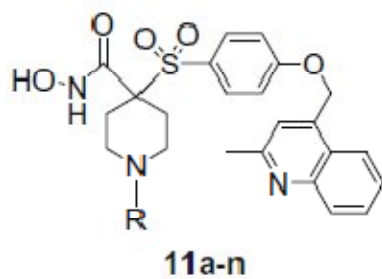
S.NO	COMPOUND	R	IC50
17	12a	BOC	3.67
18	12b	Me	1.43
19	12c	n-pentyl	1.71
20	12d	Cyclobutylmethyl	1.26
21	12e	4-PhO-Bn	2.15
22	12f	Bnb	0.97

23	12g	o-Ph-Bn	0.54
24	12h	P-Allyloxy-Bn	0.98
25	12i	3,5-Dimethoxy-Bn	2.4
26	12j	0-CF <sub>3</sub> -Bn	2.3
27	12k	m-CF <sub>3</sub> -Bn	4.4
28	12l	p-CF <sub>3</sub> -Bn	3.59
29	12m	p-Me-Bn	1.9
30	12n	p-F-Bn	3.45
31	12o	p-cl-bn	0.08
32	12p	p-meo-bn	1.18
33	12q	p-meo-bn	1.09



S.NO	COMPOUND	R1	R2	R3	IC50
34	19d	Meo	H	2-Methylpropyl	1.23
35	19e	cl	Me	2-Methylpropyl	0.3

36	19f	Me	H	p-Meo-bn	0.89
37	19g	cl	Me	p-Meo-bn	0.19
38	19h	Meo	Me	Me	0.9
39	19i	Meo	Me	Bn	0.25
40	19j	Meo	H	3,4-Methylenedioxy-bn	1.5
41	19k	Meo	Me	3,4-Methylenedioxy-bn	0.33
42	19l	Meo	H	m-Meo-Bn	2.24
43	19m	Meo	Me	m-Meo-Bn	0.28
44	19n	Meo	H	o-CF <sub>3</sub> -Bn	0.5
45	19o	Meo	Me	p-cf <sub>3</sub> -Bn	0.49
46	19p	Meo	Me	o-f-Bn	2.24
47	19q	Meo	Me	o-f-Bn	0.3
48	19r	Meo	H	m-f-Bn	0.34
49	19s	Meo	Me	p-f-bn	0.32
50	19t	Meo	Me	p-cl-bn	0.5
51	19u	cl	Me	p-cl-bn	0.33
52	19v	Meo	Me	m-CN-Bn	2.24
53	19w	Meo	Me	p-CN-Bn	0.35



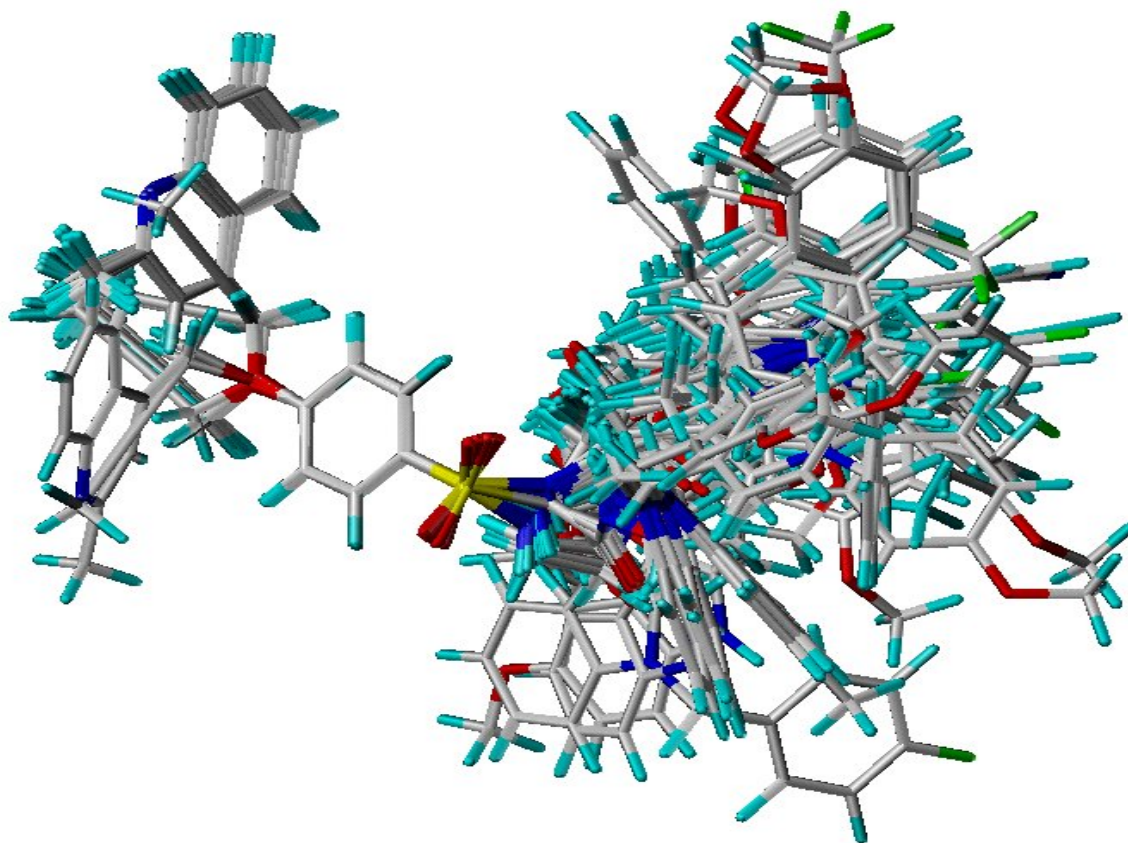
S.NO	COMPOUND	R	IC50
54	11a	H	33
55	1a	H	201
56	2a	H	1
57	11b	CHO	2
58	11c	Ac	1
59	1b	Ac	47
60	2b	Ac	2
61	11d	COiPr	2
62	11e	COPh	1
63	1c	COPh	73
64	2c	COPh	1
65	11f	CO-4-Py	2
66	11g	Boc	1
67	1d	Boc	134
68	2d	Boc	2



69	11h	CONHEt	2
70	11i	CONHEt2	3
71	11j	Me	11
72	11k	CH2-4-Py	9
73	11l	CH2Ph-3,4-Cl	65
74	1e	CH2Ph-3,4-Cl	149
75	11m	SO2Me	1.2
76	11n	SO2iPr	10

## Alignment

Alignment is the important area where the super imposition of the molecules is done. Based on the alignment the energy calculations of CoMFA\CoMSIA take place. CoMFA and CoMSIA studies require that the 3D structures of the molecules to be analyzed are aligned according to a suitable conformational template, which is assumed to be a bioactive conformation. The template molecule was taken and the rest of the molecules were aligned to it using the DATABASE ALIGNMENT option in the SYBYL. Alignment is done based on the most active molecule. All the 76 molecules get superimposed on the selected most active molecule



## RESULTS

### CoMFA and CoMSIA analysis:

PLS analysis results based on least-squares fit are listed in table 2 and 3 which shows that all the statistical indexes.

Training set values for CoMFA/CoMSIA and Docking Score

COMPOUND	PIC 50	COMFA VALUES		COMSIA VALUES		DOCKING SCORES
		PREDICTED VALUES	RESIDUAL VALUES	PREDICTED VALUES	RESIDUAL VALUES	
1	5.435	5.605	-0.17	5.763	-0.328	-24.3
2	5.844	5.907	-0.063	5.551	0.293	-22.6

3	5.47	5.553	-0.083	5.821	-0.185	-22.8
4	5.767	5.9	-0.133	5.541	0.226	-25.4
5	5.903	5.801	0.102	5.751	0.152	-23.7
6	5.667	5.668	-0.001	5.924	-0.257	-27.5
7	6.013	5.794	0.219	5.509	0.504	-29.8
8	6.008	5.89	0.118	5.636	0.372	-24.4
9	5.638	6.185	-0.547	5.772	-0.134	-24.4
10	5.356	5.722	-0.366	5.887	-0.531	-23
13	5.721	5.949	-0.228	5.928	-0.207	-28.1
14	5.462	6.152	-0.69	5.863	-0.401	-21.7
16	5.928	5.763	0.165	5.888	0.04	-22.1
17	5.086	6.099	-1.013	6.437	-1.351	-27.7
18	5.596	6.107	-0.511	6.005	-0.409	-34
19	6.552	6.109	0.443	5.878	0.674	-31.4
24	6.124	5.771	0.353	5.855	0.269	24.1
29	6.2	6.216	-0.016	6.304	-0.104	-25.9
31	5.804	6.024	-0.22	5.84	-0.036	-23.7
32	5.91	6.17	-0.26	6.143	-0.233	-22.1
34	6.05	6.168	-0.118	6.178	-0.095	-23.3
35	6.721	6.293	0.428	6.761	0.543	-28.3

37	6.602	6.102	0.5	5.841	-0.159	18.6
38	5.823	6.025	-0.202	6.318	-0.018	-23.6
39	6.481	6.621	-0.14	6.18	0.163	-25.2
40	5.649	6.186	-0.537	6.303	-0.531	-24.6
42	6.301	6.523	-0.222	6.045	-0.002	-19.5
43	5.819	6.064	0.245	5.905	0.264	-23.3
44	5.649	5.981	-0.332	6.625	-0.256	-23.6
45	6.522	6.545	-0.023	6.436	-0.103	-25.1
46	6.468	6.194	0.274	6.536	0.032	-23.8
47	6.494	6.39	0.104	6.35	0.004	-27.1
48	6.537	6.178	0.359	6.331	-0.288	-25.2
49	6.481	6.247	0.234	7.769	0.087	-21.4
50	6.387	6.303	0.084	6.609	1.281	-24.9
51	6.327	6.306	0.021	7.719	-0.038	-26.5
52	7.481	8.183	-0.702	8.736	0.488	-21
53	6.696	7.287	-0.591	8.512	0.21	-29.1
54	5.702	7.351	1.649	7.117	-0.316	-26.4
55	8.698	8.556	0.142	8.902	-0.987	-28.2
56	8.997	8.595	0.405	7.003	0.897	-29.1
57	7.327	6.956	0.371	7.098	0.78	-26.6

58	8.698	8.915	-0.217	9.014	-0.345	-26.9
59	8.836	8.563	0.073	8.335	0.363	-33.8
60	9	8.847	0.153	8.058	0.942	-35.7
61	7.136	7.344	-0.208	7.424	-0.288	-27.5
62	9	8.985	0.015	8.837	0.163	-27.5
63	8.698	8.707	-0.009	7.531	1.167	-32.3
64	6.872	6.948	-0.076	7.62	-0.748	-24.4
65	8.698	8.923	-0.225	7.864	0.834	-12.5
66	8.698	8.733	-0.035	8.32	0.378	-29.9
67	8.522	8.58	-0.058	8.573	-0.051	-33.3
68	7.958	7.913	0.045	8.174	-0.216	-33.4
69	8.045	7.893	0.152	6.979	1.066	-32.1
70	1.187	7.222	-0.035	8.076	-0.889	-28.8
71	6.69	6.675	0.0151	7.329	-0.503	-28.1
72	8.92	8.987	-0.067	8.972	-0.052	-26.1

### Test set values for CoMFA/CoMSIA and Docking Score

COMPOUND	PIC 50	COMFA VALUES		COMSIA VALUES		DOCKING SCORES
		PREDICTED VALUES	RESIDUAL VALUES	PREDICTED VALUES	RESIDUAL VALUES	
8	6.27	5.43375	0.84	6.002	0.27	-21.6
12	5.44	6.169	0.72	5.892	-0.45	-22.7
15	7.1	5.786	1.32	5.791	1.31	-24.5
20	6.85	5.0806	1.77	5.007	1.85	-29.7
21	6.44	6.16	0.28	6.058	0.39	-24
27	5.81	6.67	0.86	6.38	-0.57	-24.3
28	5.79	6.466	0.67	6.176	-0.38	-24
30	5.53	6.23	0.7	6.804	-1.27	-30.6
33	6.52	5.8711	0.65	6.025	0.49	-18.3
36	6.05	6.8623	-0.81	6.606	-0.55	-26.4
41	6.55	5.988	0.57	6.755	-0.2	-23.6
73	8	8.98	-0.98	9.257	-1.25	-25.5

All the CoMFA models have been validated using test set of 12 compounds for which results are given in ABOVE .The data set consists the results of CoMFA CoMSIA based on QSAR which are tabulated. It shows the details of q<sup>2</sup>, r<sup>2</sup>number of components-value, standard error estimate, cross validation, boot-strap values

### Data set results for CoMFA and CoMSIA

Component	COMFA		COMSIA	
q <sup>2</sup>	0.861		0.776	
r <sup>2</sup>	0.844		0.987	
N	5		6	
F-value	482.776		628.811	
SEE	0.181		0.145	
CV	0.844		0.759	
Boot-strap	Mean	Std. Dev	Mean	Std. Dev
SEE	0.140	0.083	0.140	0.058
r <sup>2</sup>	0.987	0.004	0.976	0.005

q<sup>2</sup> – leave one out- cross validated correlation co-efficient,

r<sup>2</sup> - non-cross-validated correlation co-efficient,

N- number of components used in the PLS analysis,

SEE- standard error of estimation,

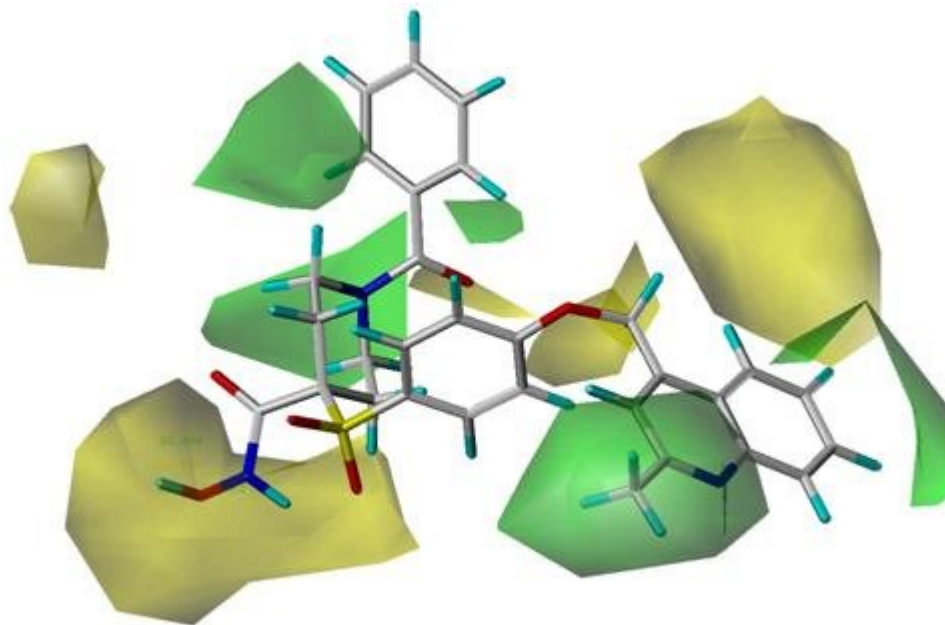
f-value, F- statistic for the analysis

### Contour analysis

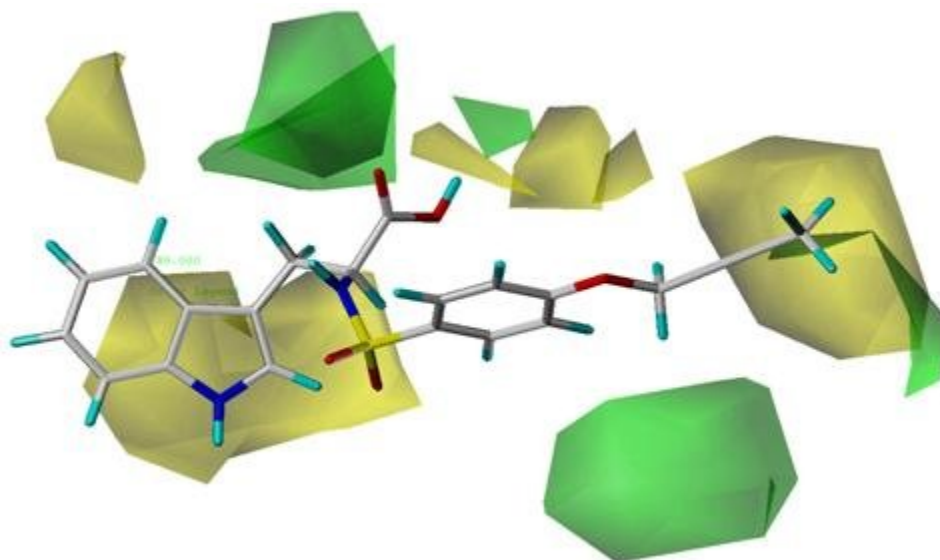
In CoMFA method, results are presented as contour maps that correlate the change in biological activity with the molecular field values. The steric contour maps are represented in green and yellow colors while the electrostatic contours are depicted in red and blue colors. The green contours are indicative of favorable regions for sterically bulkier groups and the yellow contours are indicative of regions that are sterically less favorable. Similarly, the electrostatic red plots show the regions where the presence of a negative charge is expected to enhance the activity whereas the blue contours are indicative of regions where introducing or keeping positive

charges are expected to improve the observed activity. Thus, these contour maps act as the guidance source to for the design of new molecules from the existing ones, with improved biological activity.

1. CoMFA: Steric contour map for most active compound.



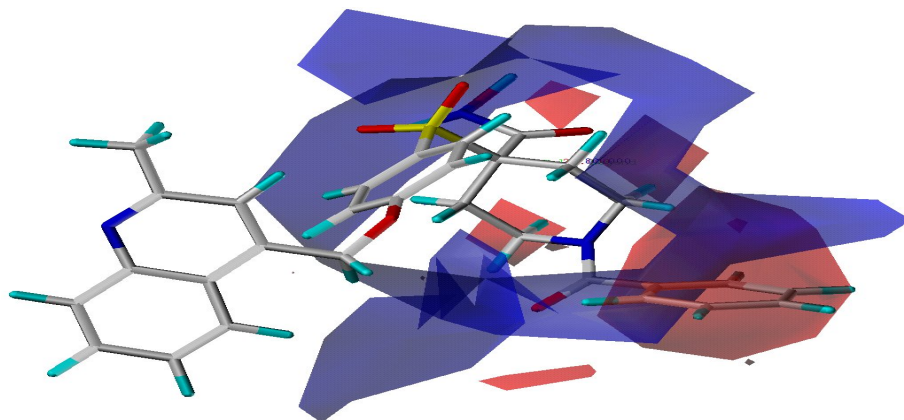
2. CoMFA: Steric contour map for least active compound.



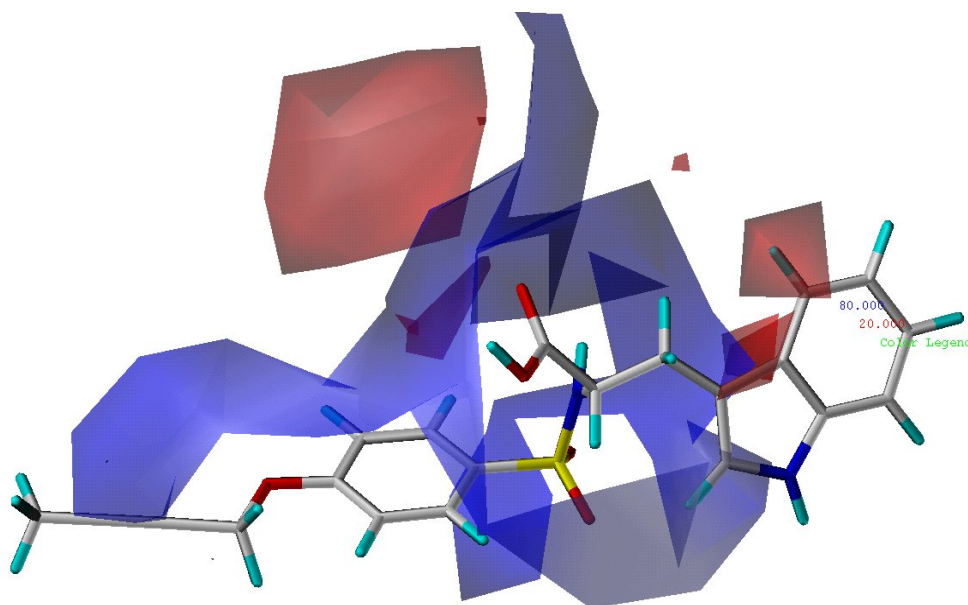
In the steric counter map: green=favoured region; yellow=disfavoured region



3. CoMFA: Electrostatic contour map for most active compound.,

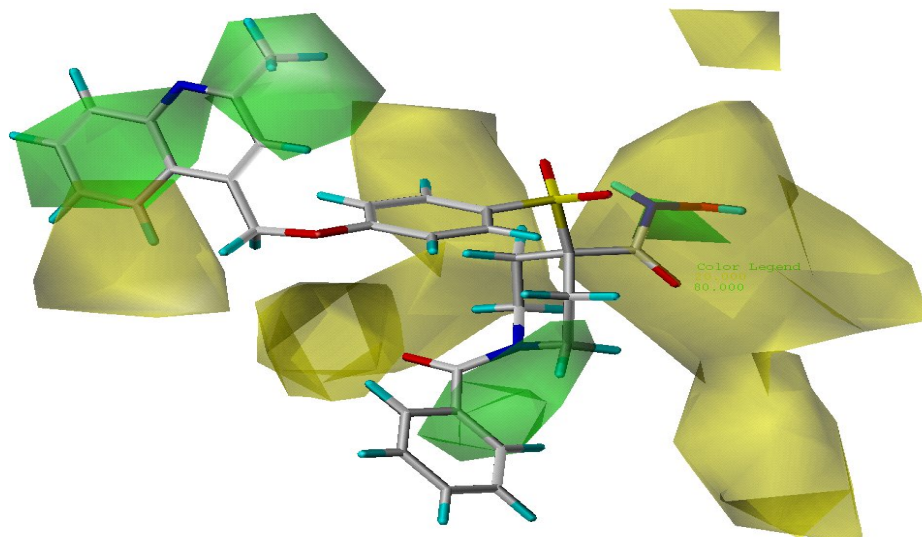


4. CoMFA: Electrostatic contour map for least active compound.

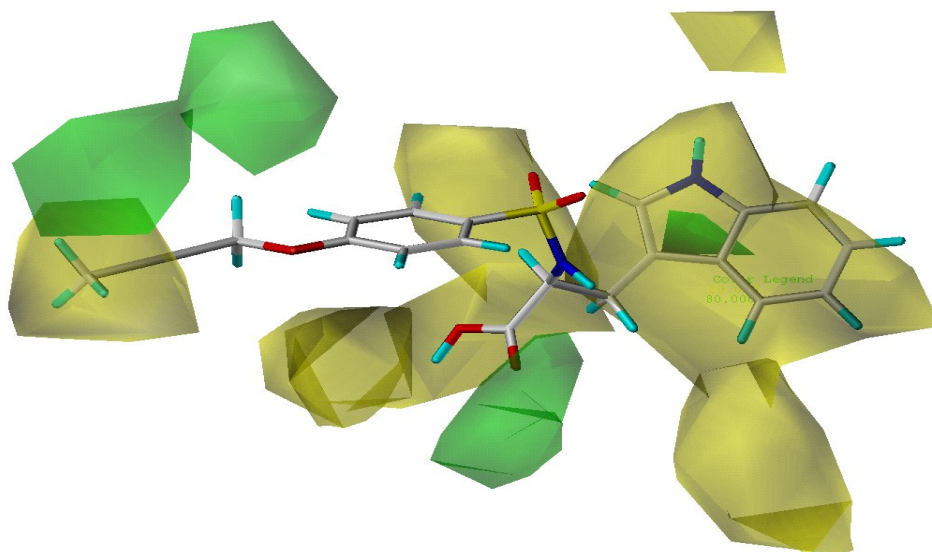


Blue=favoured region; red=disfavoured region

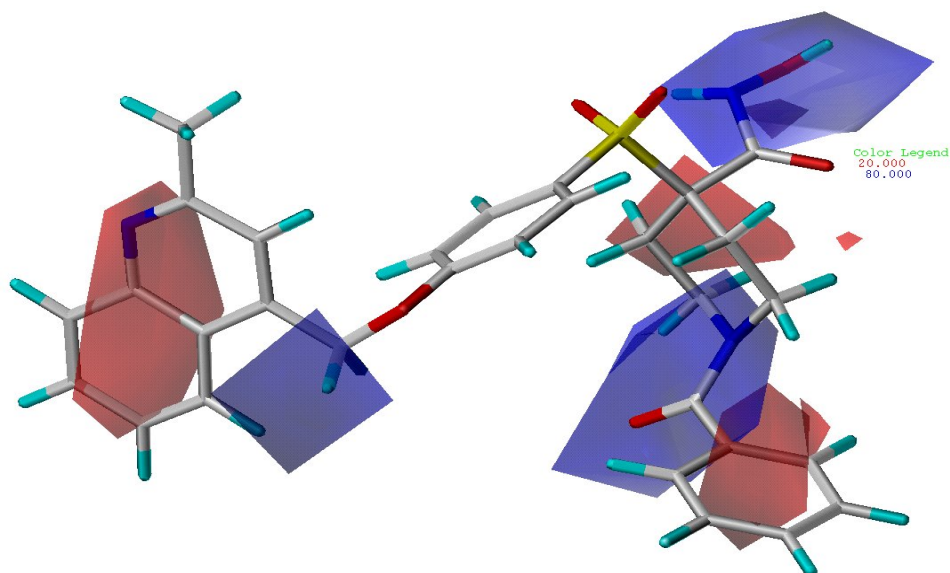
5.CoMSIA: Steric contour map for most active compound



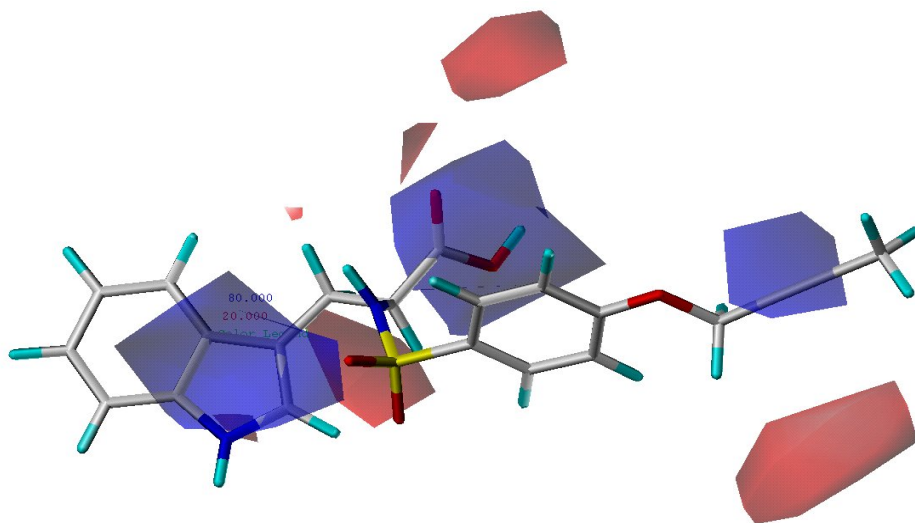
6.CoMSIA: Steric contour map for least active compound.



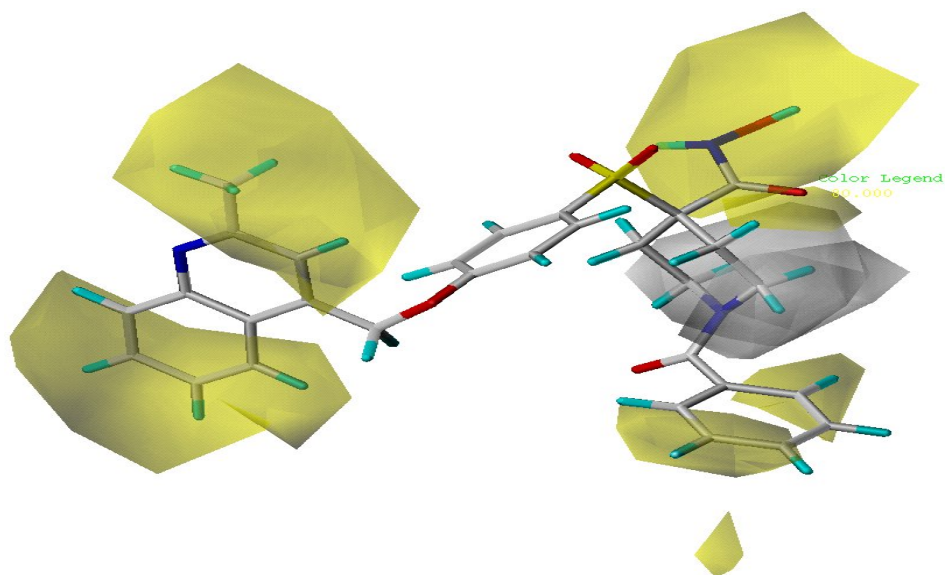
7. CoMSIA: Electrostatic contour map for most active compound.



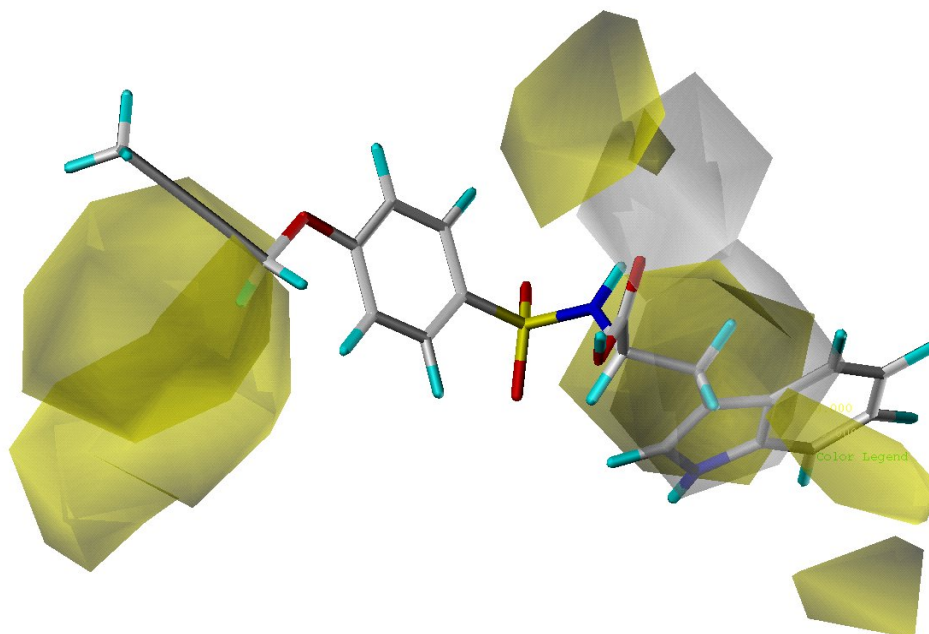
8. CoMSIA: Electrostatic contour map for least active compound.



9.CoMSIA: Hydrophobic contour map for most active compound.

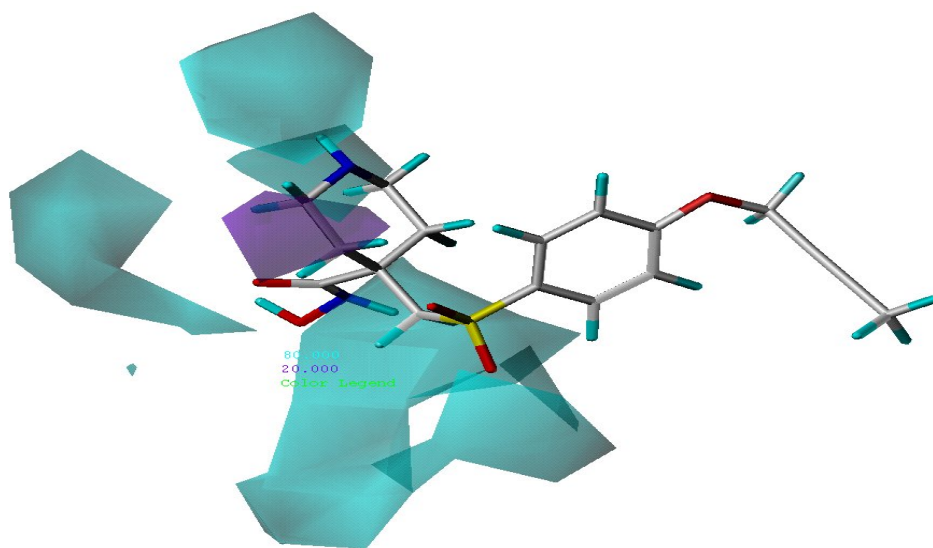


10.CoMSIA: Hydrophobic contour map for least active compound.

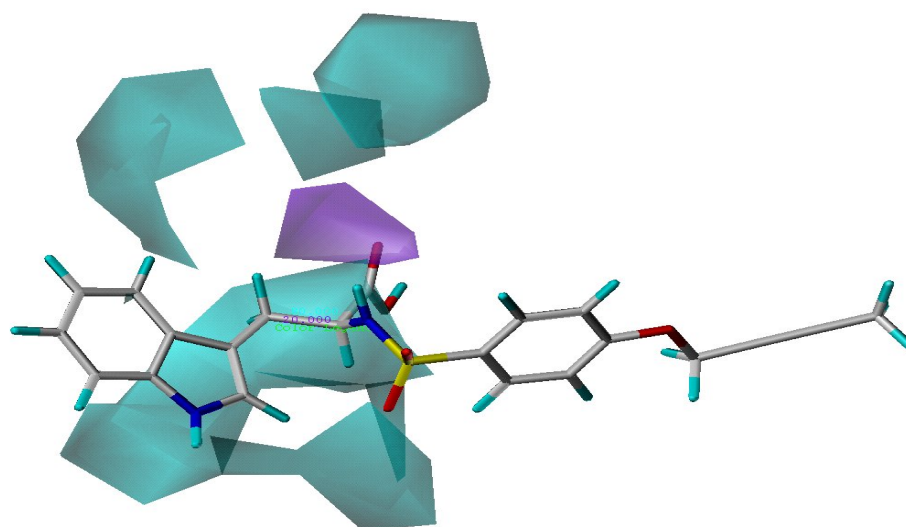


Yellow=favored region, white=disfavoured region

11.CoMSIA: Donor contour map for most active compound.



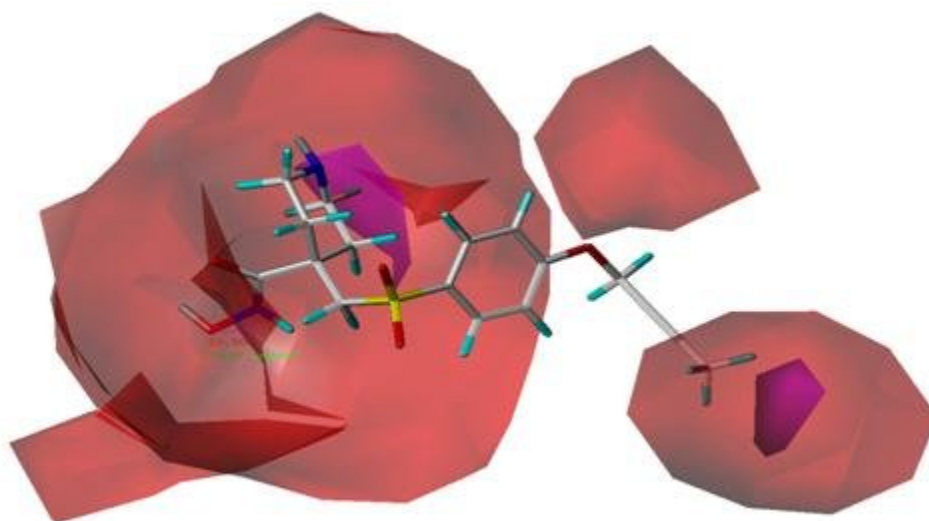
12.CoMSIA: Donor contour map for least active compound.



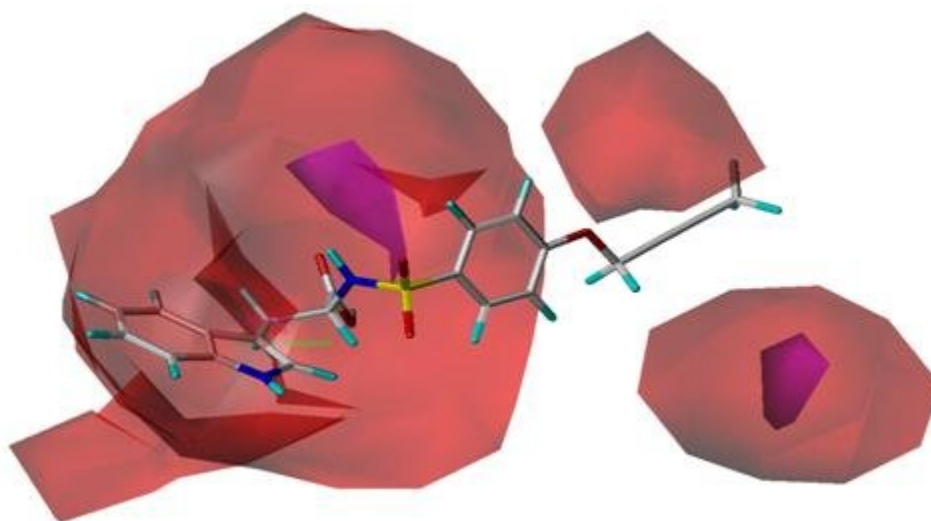
Cyan=favoured region; purple disfavoured region



13. CoMSIA: Acceptor contour map for most active compound.

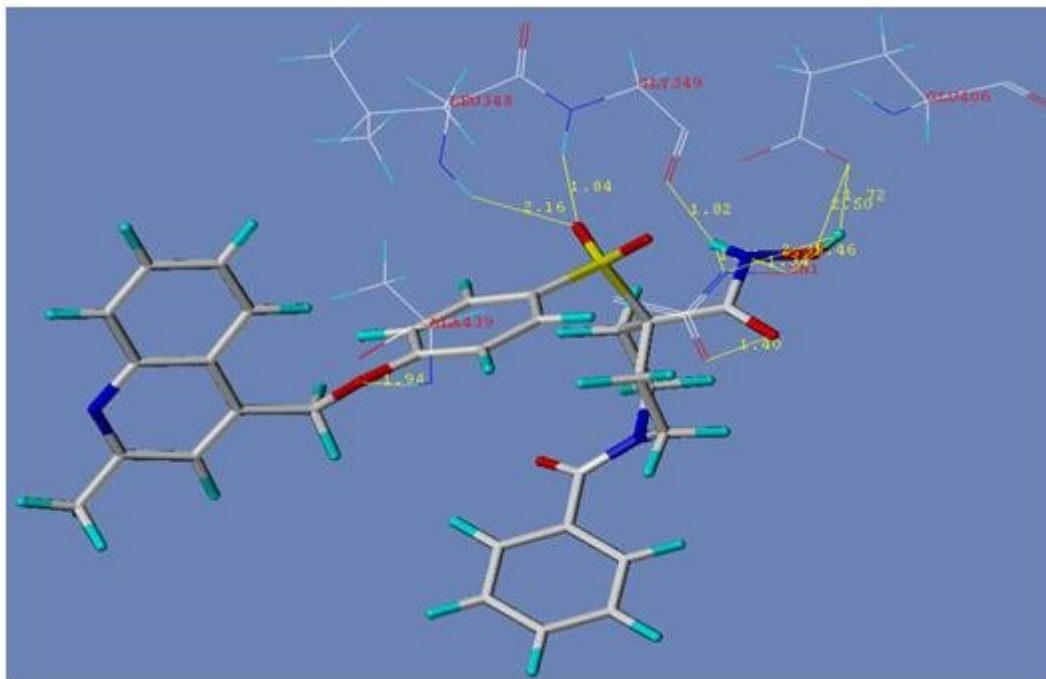


14. CoMSIA: Acceptor contour map for least active compound.

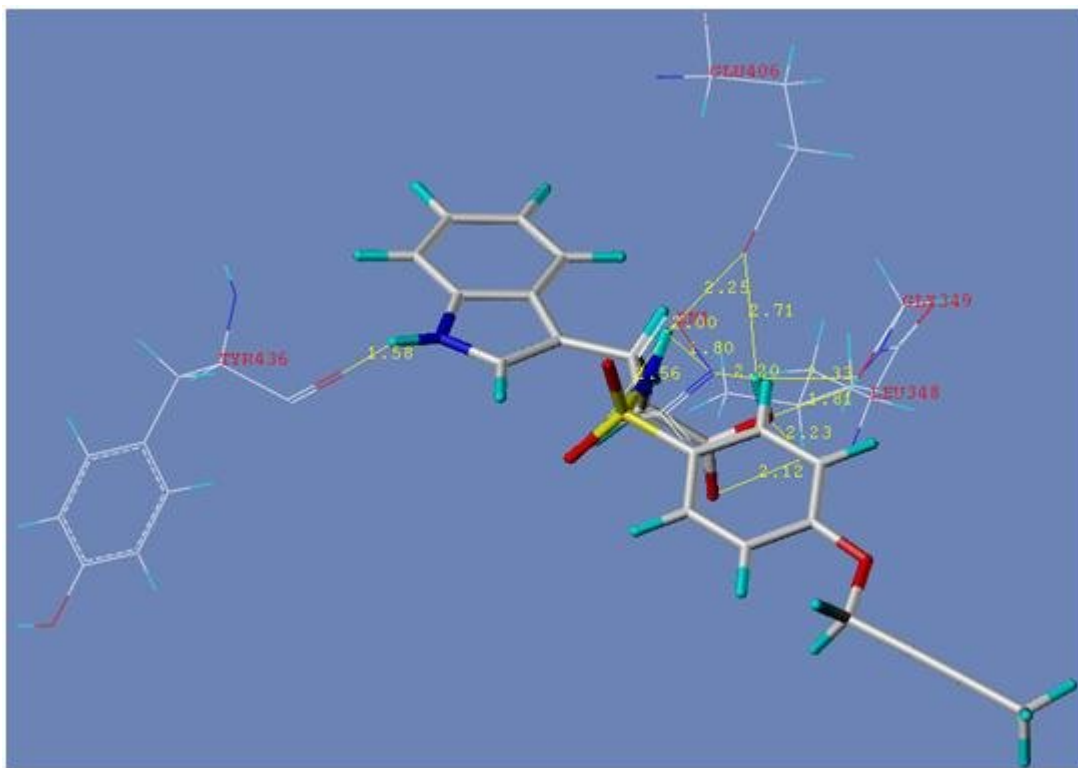


Red=favoured region; violet=disfavoured region.

## DOCKING RESULTS



Amino acid	No of Interactions	Distance (Å)
LEU 348	2	2.16
GLY 349	2	1.82
GLU 406	2	2.50
ALA 439	1	1.94
ZN1	2	1.34



Amino acid	No of Interactions	Distance (Å)
GLU 406	2	2.71
GLY 349	2	2.33
LEU 348	1	1.81
TYR 436	1	1.58
ZN1	2	2.00

## CONCLUSION

The 3D-QSAR analysis, CoMFA, and CoMSIA have been applied to a set of EGFR antagonists. The biological activity, negative logarithm pIC<sub>50</sub> was used as a dependent variable. Statistically significant models with good correlative and predictive power for anti-EGFR activities were obtained. The initial geometry of the template molecule (17th, the most active molecule of the series) was obtained and was then used to derive remaining structures. The comparison of



CoMFA and CoMSIA models revealed that the combination of electrostatic, hydrophobic, and hydrogen bond donor fields in CoMSIA gave the best results. Results of this study may be utilized for future drug design studies and synthesis of more potent anti-EGFR agents.

## REFERENCES

1. Williamson, AR. Creating a structural genomics consortium, *Nat Struct Biol*, 2000, 7(11s): 953.
2. Venclovas, C., Margelevicius, M, Comparative modeling in CASP6 using consensus approach to template selection, sequence-structure alignment, and structure assessment, *Proteins*, 2005, Vol. 61 Suppl 7: 99-105.
3. Dalal, S., Balasubramanian, S., Regan, L, Transmuting alpha helices and beta sheets, *Fold Des*, 1997, Vol. 2(5): R71-9.
4. Dalal, S., Balasubramanian, S., Regan, L, Protein alchemy: changing beta-sheet into alpha-helix, *Nat Struct Biol*, 1997, Vol. 4(7): 548-52.
5. Muckstein, U., Hofacker, IL., Stadler, PF, "Stochastic pairwise alignments" *Bioinformatics*, 2002, Vol. 18 Suppl 2: S153-60.
6. Rychlewski, L., Zhang, B., Godzik, A, "Fold and function predictions for *Mycoplasma genitalium* proteins" *Fold Des*, 1998, Vol. 3(4): 229-38.